Q-SPECIES IN ALKALI-DISILICATE GLASSES

JAN MACHÁČEK, ONDREJ GEDEON

Department of Glass and Ceramics
Institute of Chemical Technology Prague
Technická 5, 166 28 Prague
Czech Republic

E-mail: Jan.Machacek@vscht.cz

Submitted February, 26, 2003; accepted April 16, 2003

Keywords: Alkali silicate glass, Molecular dynamics, Structure

Glasses of composition $M_2O{\cdot}2SiO_2$ (M = Li, Na, K, Rb and Cs) were obtained by means of molecular dynamics simulation. The structures of these glasses were analyzed with help of Q-species distribution. The influence of alkali oxide on a decay of Q-species is monitored according to the equation $2Q^n \leftrightarrow Q^{n-1} + Q^{n+1}$. Equilibrium constant of this equation is defined by the relation $k_n = [Q^{n-1}][Q^{n+1}]/[Q^n]^2$. It was found that k_3 is decreasing in sequence Li > Na > K so that the decay of Q^3 is preferred for smaller alkali ions. Systems with higher k_3 tend to create the silicate-rich regions (abundant in Q^4) and alkali-rich regions where alkali ions are spread among chain-like structures formed by Q^2 units. For larger alkali size, k_3 increases as K < Rb < Cs. This phenomenon is probably caused by slower relaxation of simulated glasses with a large alkali ion.

INTRODUCTION

Glass, in contrary to crystals, lacks long-range translation symmetry so that standard experimental scattering methods such as X-ray or neutron scattering must be improved and/or sophisticated both theoretically and experimentally to obtain comparable results. However, scattering experiments are not able to provide 3D image of the structure but only its 1D projection resulting in the so-called radial distribution function (RDF). RDF makes possible (although not unambiguously) to determine short-range arrangement in glass structure. This short-range order (SRO) is approximately described by RDF up to 3.3 Å [1]. Unfortunately, many glass properties are associated with medium-range order (MRO) which ranges from 3.3 Å up to approximately 10 Å (figure 1). Exploration of MRO in silicate glasses may be conveniently performed by means of Q-species and their distributions [2]. Distributions of Q-species are experimentally available by nuclear magnetic resonance methods [3 - 9] and Raman spectroscopy [10 - 12]. Q^n distinguishes silicon atoms according to the number n of coordinated bridging oxygens (BO), i.e. Q^4 stands for the silicon coordinated by four BO, Q^3 corresponds to three BO and one non-bridging oxygen (NBO), etc. In silica glass all oxygen atoms are assumed to be BO. By introducing alkali oxides into silica structure some Si-BO-Si interconnections are broken and new bonds of Si-NBO type are created. The Q-species distributions of alkali ions in silicate structures generally depend on species of alkali ion and the temperature (above Tg) [5, 10, 13]. Smaller alkali ions tend to form alkali-rich regions, what may result in the increasing amount of Q^2. In these alkali-rich regions, chain-like structures of Q^2 are assumed, while Q^4 dominate in silica-rich regions [2, 4, 8]. On contrary, larger ions are rather uniformly distributed, so that Q^3 species (sheet-like structures) are preferred in such glass.

Q-species balance equation (1)

$$2\mathrm{Q}^n \leftrightarrow \mathrm{Q}^{n-1} + \mathrm{Q}^{n+1}, \quad n = 1, 2, 3 \tag{1}$$

favours number of Q^3 with increasing size of alkali ion (from Li to K) [14]. Equilibrium constant of the equation (1) is defined as

$$k_n = \frac{\left[\mathrm{Q}^{n-1}\right] \cdot \left[\mathrm{Q}^{n+1}\right]}{\left[\mathrm{Q}^{n}\right]^2} \tag{2}$$

This paper presents an investigation of Q-species in disilicate glasses, obtained by MD. Alkali disilicate glasses are excellent model systems enabling to confront new experiments (many experimental results were published [4, 5, 7, 10, 11, 13]) with simulation approaches and/or physical and chemical theories in glass. According to our knowledge, no molecular dynamics (MD) simulation of influence of alkali ions (from Li up to Cs) on distribution of Q-species in alkali disilicate glasses was published.

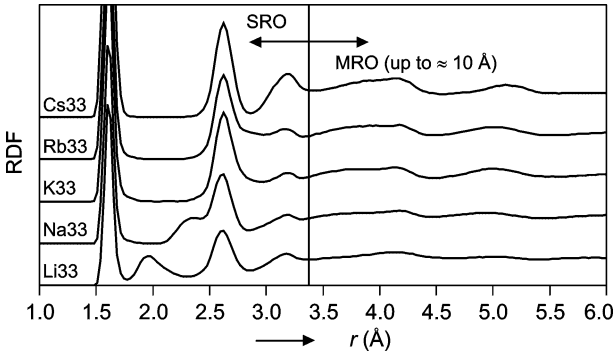

Figure 1. Total RDF of alkali disilicate glasses (MD simulation, $M_2O{\cdot}2SiO_2$). While SRO is very specific for the particular glass and discloses a lot about the coordination of atoms, MRO looks very similarly in all presented glasses.

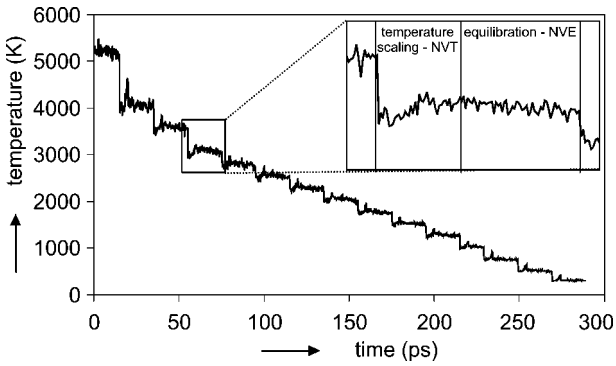

Figure 2. Cooling curve of Na33 glass. An embedded picture shows two regimes of the simulation; the first one demonstrates temperature scaling (3250 K in this case), and the second one demonstrates the following equilibration of the system.

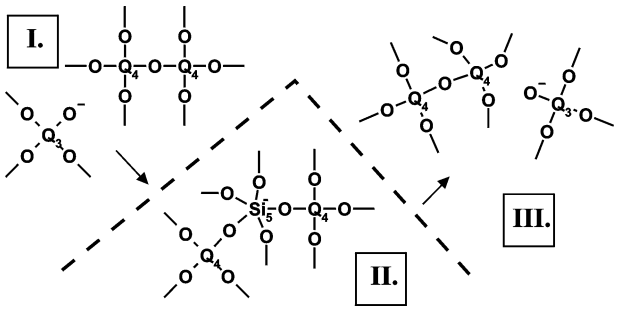

Figure 3. A scheme suggesting a formation of $Si^{(5)}$ during ionic diffusion in a silicate melt (a migrating alkali ion is not shown). In the stage I, Q^3 reacts with Q^4 yielding Q^4 and the unstable $Si^{(5)}$ (stage II). In the stage III, $Si^{(5)}$ is decomposed into Q^4 again and another Q^3 is formed.

COMPUTATIONAL DETAILS

Amorphous disilicates $M_2O{\cdot}2SiO_2$ (M = Li, Na, K, Rb, Cs) were studied, (hereafter referred as Li33, Na33, K33, Rb33 and Cs33 glasses). The MD simulations were performed by means of DL_POLY program [15]. Interatomic interactions were described by Buckingham short-range potential and the long-range Coulomb potential with full Ewald summation. The potential parameters (including ionic charges) are summarised in table 1. BKS potential [16] for Si-O and O-O pair interactions was used. This potential was originally derived from ab-initio calculations and successfully describes interactions between ions in silica polymorphs [16]. Recently, BKS potential was employed in MD simulations of silicate glasses with promising results [8, 13, 17]. A short-range cut-off was set to 7.6 Å in our simulation. A cubic computational box with periodic boundaries was used. Newton's equations of motion were numerically integrated by the leap-frog algorithm with time step of 2 fs. The time step of lithium system was decreased to 1 fs to take into account lithium low weight, but the total number of time steps was proportionally increased to retain the same total computing time. All studied systems comprised the same number of particles, i.e. 1494. MD simulation started from a random configuration at 5 000 K. The following cooling was performed with a constant volume, corresponding to the experimental density of the 300 K system (table 2).

Table 1. Potential parameters A_{ij}, ρ_{ij}, C_{ij} as used in the current MD simulations. Values for Li-Li, K-K, Rb-Rb and Cs-Cs were obtained by Ab-initio calculations performed for two ions. Values for Si-Si and Si-M were set to zero. Non-integer charges z_{Si}, z_O and z_M were 2.4, -1.2 and 0.6, respectively.

	A_{ij} (eV)	ρ_{ij} (Å)	C_{ij} (eVÅ^6)
O-O[16]	1388.773	0.36232	175.00
Si-O[16]	18003.7572	0.2052	133.5381
Li-O[22]	12120.826	0.176020	1.6624
Na-O[17]	34000.76	0.1875	10.00
K-O[22]	20510.758	0.233726	51.49
Rb-O[22]	41947.227	0.225199	52.522
Cs-O[22]	32089.737	0.267191	249.24
Li-Li	1082.01	0.148170	0.00
Na-Na[17]	9500.00	0.23	0.00
K-K	3653.467	0.308369	0.00
Rb-Rb	4225.8798	0.34579	0.00
Cs-Cs	4000.00	0.384615	0.00

Table 2. Density of simulated glasses.

	density (g/cm^3)
Li33	2.347
Na33	2.49
K33	2.46
Rb33	3.28
Cs33	3.58

The cooling procedure was performed by decrease of temperature in 330 000 time steps (660 000 time steps for Li33). The change of temperature was step-like, followed by its scaling (in Berendsen thermostat for 2500 time steps) and successive equilibration (as NVE ensemble for 7500 time steps). The cooling curve of the Na33 glass is displayed in figure 2. The final temperature was 300 K.

RESULTS

Q-species were determined from the simulated systems by the following way. All oxygen atoms coordinated by two silicon atoms within radius 2.2 Å (the first local minimum of RDF of Si-O) were considered as BO. Table 3 shows NBO and BO distributions in five simulated glasses. Only small differences, compared with stoichiometry (40 % NBO and 60 % BO), can be found. Afterwards, coordination numbers were determined for silicon atoms (table 4) as the number of oxygens up to 2.2 Å. Simulated glasses contain small amount of five-coordinated silicon $Si^{(5)}$ (about 5 %.). Appearance of $Si^{(5)}$ particles is very common phenomenon in MD simulations with pair-wise atomic potential. On that account, many-body potentials are often used for MD simulations of silicate glasses [18]. Although BKS potential is pair-wise potential, the results obtained are almost excellent [17]. In addition, it seems that $Si^{(5)}$ exist in molten silicates and plays an important role in diffusion of ions [19].

Table 3. The relative abundance (in %) of oxygen atoms with various coordination numbers (crn) in the simulated glasses, i.e. 0 stands for free oxygen anion, 1 for NBO, 2 for BO, and 3 corresponds to trigonal oxygen.

crn	Li33	Na33	K33	Rb33	Cs33
0	0.12	0.12	0	0	0
1	37.83	37.83	37.71	37.95	39.28
2	61.81	61.81	62.29	62.05	60.6
3	0.24	0	0	0	0

Huge amount of $Si^{(5)}$ in simulated glasses can be attributed to the extremely high cooling rates. In table 5, Si atoms are distinguished according to their coordination number and the number of BO in their first coordination shell. $Si^{(5)}$ were decomposed using the following idea. $Si^{(5)}$ particle may act in the ionic diffusion (figure 3) as reported in the model suggested in [19]. If one assumes all $Si^{(5)}$ to be intermediate states the suggested schemes can be used

$$Si^{(5)5} + Q^4 \rightarrow Q^4 + Q^3$$
$$Si^{(5)4} + Q^4 \rightarrow Q^3 + Q^3$$
$$Si^{(5)3} + Q^4 \rightarrow Q^2 + Q^3$$

where $Si^{(5)n}$ is the five-coordinated silicon with n BO. Figure 3 demonstrates the decomposition according to the first scheme, i.e. formation of Q^3 and Q^4 from Q^4 and $Si^{(5)5}$. As consequence of all of these schemes, NBO converts to BO. An analysis of the simulated glasses confirmed, that the number of $Si^{(5)}$ particles corresponds to the difference between the number of NBO and the number of alkali ions. Hence, the suggested decomposition of $Si^{(5)}$ properly corrects the number of NBO and enables to involve all Si into Q-species analysis. The corrected distribution of Q-species is presented in the figure 4. Several starting configurations were used to study their influence to the final Q-species distributions. However, no significant effect was found. In addition, the number of particles in the simulated box was lowered down to 900. Although some authors report changes in distributions of Q-species [13], no changes were recognized in results obtained with the decreased number of particles. Equilibrium constants k_2 and k_3 were calculated according the equation (2) for 300 K and are displayed in figure 5.

Table 4. The relative abundance (in %) of four- and five-coordinated silicon atoms in simulated glasses.

crn	Li33	Na33	K33	Rb33	Cs33
4	94.58	94.58	94.28	94.88	98.8
5	5.42	5.42	5.72	5.12	1.2

Table 5. The fraction of silicon atoms (in %) distinguished according to BO and their coordination. The number in the first column corresponds to the number of BO in the first coordination shell of Si. $Si^{(4)}$ and $Si^{(5)}$ stand for four- and five-coordinated silicon.

	Li33		Na33		K33		Rb33		Cs33	
n(BO)	$Si^{(4)}$	$Si^{(5)}$	$Si^{(4)}$	$Si^{(5)}$	$Si^{(4)}$	$Si^{(5)}$	$Si^{(4)}$	$Si^{(5)}$	$Si^{(4)}$	$Si^{(5)}$
0	0.3	0	0	0	0	0	0	0	0	0
1	6.02	0	3.01	0	3.92	0	2.41	0	1.51	0
2	19.28	0	20.48	0	16.87	0	19.88	0	24.1	0
3	35.84	0.3	45.18	0	48.19	0	47.89	0	45.48	0
4	33.13	0.3	27.11	0.6	25.3	0.6	24.7	0	27.71	0
5	0	4.82	0	3.61	0	5.12	0	5.12	0	1.2

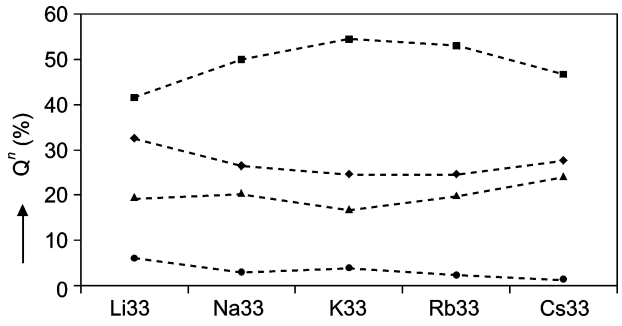

Figure 4. Distribution of Q-species (■ Q^3, ◆ Q^4, ▲ Q^2, ● Q^1) in the simulated glasses. Dashed lines serve as guides for an eye.

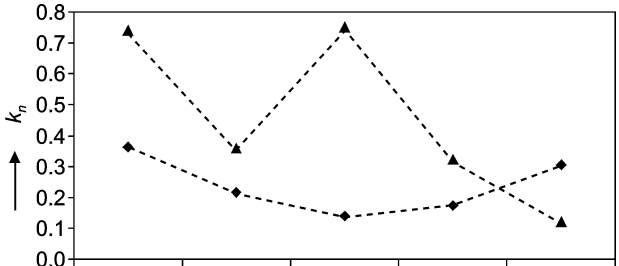

	Li33	Na33	K33	Rb33	Cs33
-▲- k_2	0.74	0.36	0.75	0.32	0.12
-◆- k_3	0.36	0.22	0.14	0.17	0.31

Figure 5. Dependence of equilibrium constants k_2 and k_3 on an alkali ion kind. Dashed lines serve as guides for an eye.

DISCUSSION

The constant k_2 shows large variations with the kind of the simulated alkali disilicate. Except for K33 glass, k_2 decreases (number of Q^2 increases) with larger alkali ion. However, such result is not, due to the poor statistics of Q^1 and Q^2 (in contrary to k_3), well established. k_3 variation with alkali species is not monotonous, as one could expect on base of experimental data [14], which are also supported by the simple model stating that k_3 decreases with alkali ion size. K33 glass has the least value of k_3 and therefore the highest fraction of Q^3. On the other hand, Li33 glass reveals the highest k_3. All mentioned results obtained from MD simulations are in agreement with experimental observations of many authors concerning Li-, Na- and K-glass [12, 14, 20]. The highest k_3 in lithium glass can be attributed to the highest tendency of lithium ions to form alkali-rich regions. The regions can be described by Q^2 units forming chain-like structures, around which alkali ions are located. The higher willingness of the separation into two different phases for binary alkali-silicate glass with smaller alkalis is then a consequence of their higher aggregation tendency.

Surprisingly, k_3 increases from K33 to Cs33. The difference between Rb33 and K33 is negligible in frame of the statistics. The small difference can be expected due to the closeness of the ionic radii of potassium and rubidium. However, k_3 in Cs33 glass shows statistically significant declination from K33 or Rb33. Hence, two parallel processes can be assumed in the simulated glasses: 1) alkali segregation, caused by alkali ion field strength and 2) structure relaxation during cooling of glass. The slower relaxation favours Q^3, since the fast frozen system is closer to liquid, where higher value of k_3 was observed [5, 10, 13]. The relaxation in glass containing relatively small ions can be expected to be faster than for systems with large alkalis (Cs). This idea is supported by the following simulation. The simulation with a reduced atom weight of caesium (6.9 instead of 132.9) was performed so that diffusion of Cs ions effectively increases (relaxation time of Cs decreases). Then, the value of k_3 decreased to that in Rb33 glass at room temperature.

Equilibrium constant k_3 is higher in simulated disilicates than in experimental ones. Most often it is attributed to the fast cooling rates [8, 13, 21]. However, there are still great differences among various experimental findings coming from Raman spectroscopy [11, 12], MAS-NMR [14], and more recently from 2D-NMR [19].

CONCLUSION

Five glasses of composition $M_2O{\cdot}2SiO_2$ (M = Li, Na, K, Rb, Cs) were obtained by means of molecular dynamics simulation. The structures of these glasses were analyzed with help of Q-species. The influence of kind of alkali oxide on the distributions of Q-species was studied. Q^3 species were found to be preferred in Li33 and Na33. These systems tend to create the silicate-rich (abundant in Q^4) and alkali-rich regions. On the other hand, for larger alkali size, k_3 increases as K < Rb < Cs. This phenomenon is probably caused by slower relaxation of simulated glasses with a large alkali ion. However, this assumption needs further investigation.

Acknowledgement

This work was supported by Grant Agency of the Czech Republic through the grant No 104/03/0976. It was also part of the research project CEZ: MSM 223100002 Preparation and properties of advanced materials - modelling, characterization, and technology.

References

1. Varschneya A.K.: *Fundamentals of Inorganic Glasses*, 1st ed., p.91, Academic Press, San Diego 1994.
2. Shelby J.E.: *Introduction to Glass and Technology*, 1st ed., p.79-86, The Royal Society of Chemistry, Cambridge 1997.
3. Zhang P., Grandinetti P.J., Stebbins J.F.: J.Phys.Chem. B *101*, 4004 (1997).
4. Dupree R., Holland D., Williams D.S.: J.Non-Cryst. Solids *81*, 185 (1986).
5. Maekawa H., Florian P., Massiot D., Kiyono H., Nakamura M.: J.Phys.Chem. *100*, 5525 (1996).
6. Maekawa H., Yokokawa T.: Geochim.Cosmochim. Acta *63*, 2569 (1997).
7. Selvaray U., Rao K.J., Rao C.N.R., Klinovsky J., Thomas J.M.: Chem.Phys.Letters *114*, 24 (1985).
8. Olivier L., Yuan X., Cormack A.N., Jäger C.: J.Non-Cryst.Solids *293-295*, 53 (2001).
9. Mortuza M.G., Dupree R., Holland D.: J.Non-Cryst. Solids *281*, 108 (2001).
10. You J., Jiang G., Xu K.: J.Non-Cryst.Solids *282*, 125 (2001).
11. Zotov N.: J.Non-Cryst.Solids *287*, 231 (2001).
12. Bykov V.N., Osipov A.A., Anfilogov V.N.: Phys. Chem.Glasses *41*, 10 (2000).
13. Horbach J., Kob W., Binder K.: Chem.Geol. *174*, 87 (2001).
14. Maekawa H., Maekawa T., Kawamura K., Yokokawa T.: J.Non-Cryst.Solids *127*, 53 (1991).
15. Smith W., Forester T.R., http://www.dl.ac.uk/TCSC/ /Software/DL_POLY (2000).
16. van Beest B., Kramer G. J., van Santen R. A.: Phys. Rev.Lett. *64*, 1955 (1990).
17. Yuan X., Cormack A. N.: J.Non-Cryst.Solids *283*, 69 (2001).
18. Vessal B., Amini M., Fincham D., Catlow C.R.A.: Philos.Mag. B *60*, 753 (1989).
19. Farnan I.: Curr. Opin. Solid State Mater.Sci. *3*, 371 (1998).
20. Matson. D.W., Sharma S.K., Philpotts J.A.: J.Non-Cryst.Solids *58*, 323 (1983).
21. Smith W., Greaves G.N., Gillan M.J., J. Chem.Phys. *103*, 3091 (1995).
22. Teter D.: private communication.

Q-MOTIVY VE SKELNÝCH ALKALICKÝCH DISILIKÁTECH

JAN MACHÁČEK, ONDREJ GEDEON

Ústav skla a keramiky
Vysoká škola chemicko-technologická v Praze
Technická 5, 166 28 Praha

Pomocí molekulově dynamické simulace byla získána skla o složení alkalického disilikátu $M_2O{\cdot}2SiO_2$ (M = Li, Na, K, Rb a Cs). Struktura uvedených systémů byla analyzována pomocí distribuce Q-motivů. Je sledován vliv alkalického oxidu na rozpad Q-motivů podle rovnice $2Q^n \leftrightarrow Q^{n-1} + Q^{n+1}$. Rovnovážná konstanta této rovnice byla definována vztahem $k_n = [Q^{n-1}][Q^{n+1}]/[Q^n]^2$. Bylo zjištěno, že konstanta k_3 klesá v řadě Li > Na > K. To znamená, že rozpad Q^3 motivů je upřednostněn u malých alkalických iontů. Systémy s vyšším k_3 mají sklon vytvářet oblasti bohaté na křemičitou matrici (převládá Q^4) a oblasti bohatší na alkálie, kde jsou alkalické ionty rozprostřeny v okolí řetězcových motivů Q^2. Pro větší alkalické ionty roste k_3 v řadě K < Rb < Cs. Tento jev je pravděpodobně způsoben pomalejší relaxací simulovaných skel s větším alkalickým iontem.